



# Effects of solid substrate on structure and properties of casting waterborne polyurethane/carboxymethylchitin films

Ming Zeng, Lina Zhang\*, Yuxiang Zhou

*Department of Chemistry, Wuhan University, Wuhan 430072, People's Republic of China*

Received 11 August 2003; received in revised form 6 January 2004; accepted 27 February 2004

## Abstract

We prepared two series of semiinterpenetrating polymer network (semi-IPN) films from cross-linked waterborne polyurethane (WPU) and carboxymethylchitin (CMCH) in the aqueous solution on the glass and Teflon as the hydrophilic and hydrophobic substrates, respectively, by casting method. The chemical compositions, structure and morphologies of the films were examined by attenuated total reflection Fourier transform infrared spectroscopy (ATR-FTIR) and scanning electron microscopy (SEM). The miscibility, thermal stability and mechanical properties of the films were investigated by density measurement, dynamic mechanical analysis (DMA), ultraviolet (UV) spectroscopy, thermogravimetric analysis (TGA), tensile testing and solvent swelling testing. The results revealed that the semi-IPN films exhibited good miscibility when CMCH content was lower than 35 and 65 wt% for the films prepared on the glass and Teflon, respectively, resulting in higher light transmittance, thermal stability and tensile strength than the WPU film. Interestingly, the films prepared with the Teflon as the substrate possessed better miscibility and higher storage modulus, thermal stability, tensile strength and solvent-resistance than that with the glass as the substrate over the entire composition range studied here. This difference can be attributed that a strong intermolecular interaction occurred between WPU and CMCH to form a dense architecture, owing to that two kinds of macromolecules all were repulsed from the Teflon surface and forced to concentrate into inner surface. It has been confirmed that the hydrophilicity and hydrophobicity of the solid substrate significantly influenced the structures and properties of the casting films, and using Teflon solid substrate can more effectively improve the miscibility and properties of the semi-IPN materials with hydrophilic character than glass one. We proposed a model describing the formation of WPU/CMCH semi-IPN films cast on the hydrophilic and hydrophobic substrates to illustrate the different structures of two types of films.

© 2004 Elsevier Ltd. All rights reserved.

*Keywords:* Interpenetrating polymer networks; Substrate; Interface

## 1. Introduction

Environmental friendly materials from renewable resources, such as chitin, cellulose, starch, polysaccharides, etc. have attracted much attention. Chitin, a (1 → 4)-linked polysaccharide composed of 2-acetamido-2-deoxy-β-D-glucopyranose residues, is widely distributed in nature [1]. Materials made of chitin or modified chitin have the attractive advantages of being non-toxic, biodegradable, antibacterial and with relatively good biocompatibility, which offer large unexplored commercial applications [2,3]. Carboxymethylchitin (CMCH), a water-soluble derivative of chitin, has potential applications in industry, pharmacy,

personal care, agriculture and biotechnology [4,5]. However, the CMCH film has poor toughness, so it is hardly to be accepted in practical applications. It is worth noting that waterborne polyurethanes (WPU) with good flexibility, as a non-toxic, nonflammable and environment-friendly material, allow a broad range of application areas [6,7]. These products present many features related to conventional solvent-borne polyurethanes with the advantages of presenting low viscosity at high molecular weight and good applicability [8]. However, the WPU is deficient in chemical resistance, thus a variety of room temperature curing cross-linkers have been developed to improve the performance of WPU [8,9].

Polymer blends continue to be a subject of intensive investigations because of the simplicity and effectiveness of mixing two different polymers to obtain new materials from

\* Corresponding author. Tel.: +86-27-8721-9274; fax: +86-27-8788-2661.

E-mail address: [lnzhang@public.wh.hb.cn](mailto:lnzhang@public.wh.hb.cn) (L. Zhang).

both academic and industrial views in the last decades [10]. Interpenetrating polymer network (IPN), a kind of polymer blends held together by permanent entanglement between two or more distinctly cross-linked polymers, has drawn much attention due to special properties brought about by interlocking of polymer chains [11,12]. It is especially important that semi-IPN materials provide a novel way for modification and exploitation of natural polymers. In our laboratory, semi-IPN materials from castor oil-based polyurethane and derivatives of natural polymers such as nitrokonjac glucomannan [13], benzyl konjac glucomannan [14], and nitrocellulose [15] have been synthesized. It is noted that the morphology and properties of multi-component polymers are dramatically affected by the interface with solid [16,17]. The structure, morphology and properties of an IPN material are crucial to its use in diverse fields such as adhesives, coating, optoelectronic devices and templating in lithographic process [16]. However, very little research has focused on the effect of the interface between IPN material and substrate on the resultant IPN morphology and structure [18–20].

The effects of solid substrate on structure, miscibility, morphology and properties of the semi-IPN materials from natural polymers in aqueous system have been scarcely reported. A basic understanding of the behavior for casting semi-IPN films prepared with different solid substrate is essential for a successful research and development of the new materials. In recent work, we have prepared a series of blend films from WPU and CMCH in aqueous system with the glass as the substrate [21]. The blend films have higher thermal stability and tensile strength than the WPU film, and certain degree of miscibility over the entire composition range. In this paper, we attempted to study the structure, miscibility and properties of the WPU/CMCH semi-IPN films by attenuated total reflection Fourier transform infrared spectroscopy (ATR-FTIR), scanning electron microscopy (SEM), dynamic mechanical analysis (DMA), ultraviolet (UV) spectroscopy, thermogravimetric analysis (TGA), tensile testing and solvent swelling testing. Glass and Teflon were employed as the hydrophilic and hydrophobic substrates, respectively, to clarify their effects on the intermolecular interaction between WPU and CMCH in the semi-IPN materials.

## 2. Experimental

### 2.1. Synthesis of WPU

Waterborne anionic polyurethane was prepared through a two-stage polymerization process [22]. Commercial 2,4-toluene diisocyanate (TDI) supplied by Shanghai Chemical Co. (China) was vacuum-dried at 80 °C for 2 h, and used as hard segments. Polypropylene glycol (PPG;  $M_w = 1000$ ) supplied by Nanjing Chemical Factory (China) was vacuum-dried at 105 °C for 5 h, and used as soft segments.

Dimethylol propionic acid (DMPA) supplied by Chengdu Polyurethane Co. (China) was also vacuum-dried at 110 °C for 2 h, and used as chain extender and anionic center. Triethylamine (TEA) supplied by Shanghai Chemical Co. (China) and ketone as neutralized reagent and solvent, respectively, were immersed in 3 Å molecular sieves for more than a week to dehydrate before use. The dry PPG was introduced in a three-necked flask, and heated to 75 °C with mechanical stirring, then TDI in one portion was added with the stirring to be continued at 75 °C for 2.5 h. An equivalent amount of dry DMPA was added in one portion to the mixture. The reaction was carried out for 2–3 h until the NCO groups content reached a given value, determined by dibutylamine back titration [23]. The ketone was added to reduce the viscosity of the prepolymer. Finally, the product was cooled to 60 °C, and neutralized with TEA for 30 min. The WPU was formed by dispersing in deionised water for a period of 30 min to get the solid content of the WPU to be 17 wt%.

### 2.2. Preparation of CMCH

CMCH was prepared through a modified reaction process in which NaOH amount used was lower than reported in Ref. [24]. Chitin was supplied by Zhejiang Yuhuan Sea Biochemical Co. (China), and its viscosity-average molecular weight ( $M_\eta$ ) and degree of acetylation are  $1.31 \times 10^6$  and 92.5%, respectively. It was used without further purification. Chloroacetic acid and isopropyl alcohol are analytical grade.

Mixture of chitin (10 g) and 50 wt% aqueous NaOH (20 g) was stirred for 1 h, then kept overnight at  $-18$  °C. Resulting mixture was dissolved in the isopropyl alcohol (140 ml), and the chloroacetic acid (11 g) was added into the mixture, and kept at room temperature for 2 h and at 60 °C for 2 h. The solution was neutralized with HCl at 40 °C, yielding a precipitate of CMCH. The CMCH was dissolved in water (240 ml) with the stirring for 2 h. The brown and viscous solution was centrifuged at 4000 rpm for 15 min, and the supernatant was slowly added into 500 ml acetone. The fibrous precipitate was washed with ethanol and 80 wt% aqueous ethanol, respectively. The product was dried and stored in a desiccator. The  $M_\eta$  of the resulting product CMCH was determined by the viscometry method [5] to be  $1.54 \times 10^5$ .

### 2.3. Preparation of WPU/CMCH films

One gram of CMCH was dissolved in 25 g of water to obtain 4 wt% CMCH solution. Ethylene glycol diglycidyl ether (EGDE) is analytical grade, and used as a cross-linking reagent by the amount of 5 wt% of solid content of WPU in the blend. The mixture of WPU, EGDE and CMCH solution was stirred at room temperature for 2 h to obtain a clear solution. Then the resulting solution was cast into a glass or Teflon mold, and dried under atmospheric pressure

at 25 °C for 5–7 days to yield semi-IPN films, in which CMCH linear macromolecule exist in the WPU networks, with thickness of ca. 120 μm. By changing the weight ratios of CMCH such as 15, 35, 50, 65 and 85 wt% in the blends, two series of WPU/CMCH semi-IPN films were prepared and coded as CMPE15-G, CMPE35-G, CMPE50-G, CMPE65-G and CMPE85-G on the glass, and CMPE15-T, CMPE35-T, CMPE50-T, CMPE65-T and CMPE85-T on the Teflon, respectively. Films prepared from pure CMCH and cross-linked WPU on the glass and Teflon mold, respectively, were coded as CMCH-G, CMCH-T, WPUE-G and WPUE-T.

#### 2.4. Characterization

ATR-FTIR was performed on a spectrometer (1600, Perkin–Elmer Co., USA). The samples were taken at

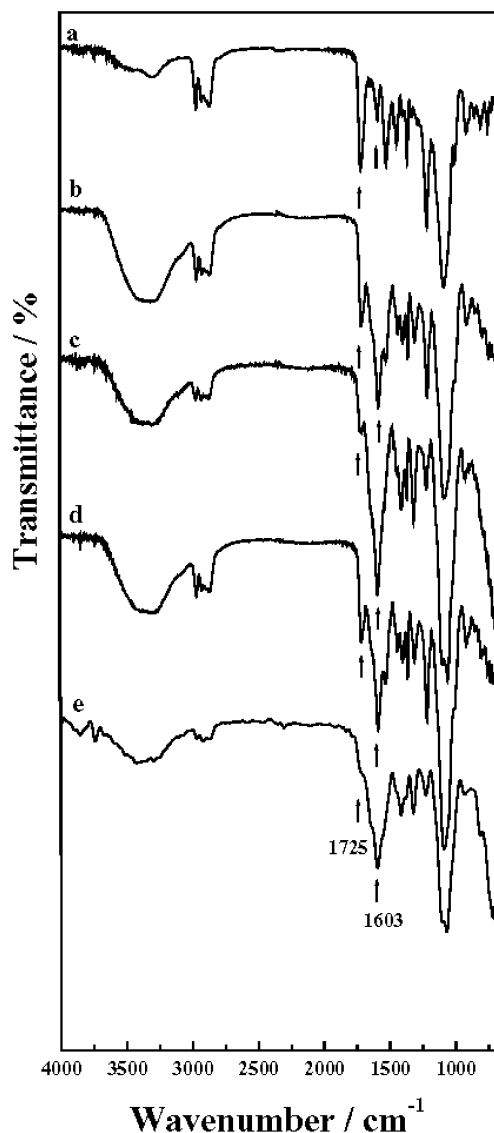


Fig. 1. ATR-FTIR spectra of the films WPUE-G (a), CMPE65-T (bottom side, b), CMPE65-T (surface side, c), CMPE65-G (bottom side, d), and CMPE65-G (surface side, e).

random from the flat films and data were collected over 16 scans with a resolution of 4 cm<sup>-1</sup> at room temperature.

The density ( $\rho$ ) of the films WPUE and CMPE were measured at 30 °C by determining the weight of a volume-calibrated psychomotor filled with a mixture of NaCl aqueous solution and distilled water, in which the samples achieved floatation level. The density of the liquid mixture equals the density of the samples. Three parallel measurements were carried out for every sample.

To study the networks structure and intermolecular interaction between WPU and CMCH, the CMPE films were extracted with water to remove the water-soluble CMCH, and then observed with SEM. The extraction of the CMPE films was performed as follows: 1 g of CMPE film enclosed in a nylon mesh was immersed in water accompanying mild stirring for 24 h at 25 °C, and then the extracted films were vacuum-dried at 40 °C for 12 h. The percentage amount of extracted CMCH was calculated by

$$\text{Extracted amount (wt\%)} = [(w_i - w_e)/w_i] \times 100\% \quad (1)$$

where  $w_i$  and  $w_e$  are weight of initial and extracted CMPE films, respectively. SEM micrographs of the films were taken with a microscope (X-650, Hitachi, Japan). The CMPE films extracted with and without water were frozen in liquid nitrogen and snapped immediately, and then vacuum-dried. The surface (contact with air), bottom (contact with solid substrate) and cross section (fracture surface) of the films were sputtered with gold, and then observed and photographed. Optical transmittance ( $T_T$ ) of the films was measured with a UV–vis spectrophotometer (Shimadzu UV-160A, Japan) at a wavelength of 800 nm. The thicknesses of films were ca. 120 μm.

DMA was carried out with a dynamic mechanical thermal analyzer (DMTA-V, Rheometric Scientific Co., USA) at 1 Hz and a heating rate of 5 °C/min in the temperature range from –50 to 200 °C. The specimens with typical size of 10 mm × 10 mm (length × width) were used. TGA of the specimens with 1 mm width and 1 mm length were carried out with a thermobalance (PRT-2, Beijing Optical Instruments Factory, China) under an air atmosphere from 25 to 600 °C, at a heating rate of 10 °C/min.

Tensile strength ( $\sigma_b$ ) and elongation at break ( $\epsilon_b$ ) of the films were measured on a versatile tester (CMT-6503, Shenzhen SANS Test Machine Co. Ltd., China) according to the ISO6239-1986 standard with a tensile rate of 5 mm/min. The size of the films was 70 mm length, 10 mm width, with 50 mm distance between two clamps. Five parallel measurements were carried out for every sample. Swelling tests of the films were performed with different solvents. The weight of the dry film ( $w_0$ ) was measured directly, and then the film was immersed into the solvent to prepare swelling sample. The solvent was covered with a watch glass to prevent evaporation. After 24 h the sample was taken out, and the excess solvent on the film was wiped off. The degree of swelling was

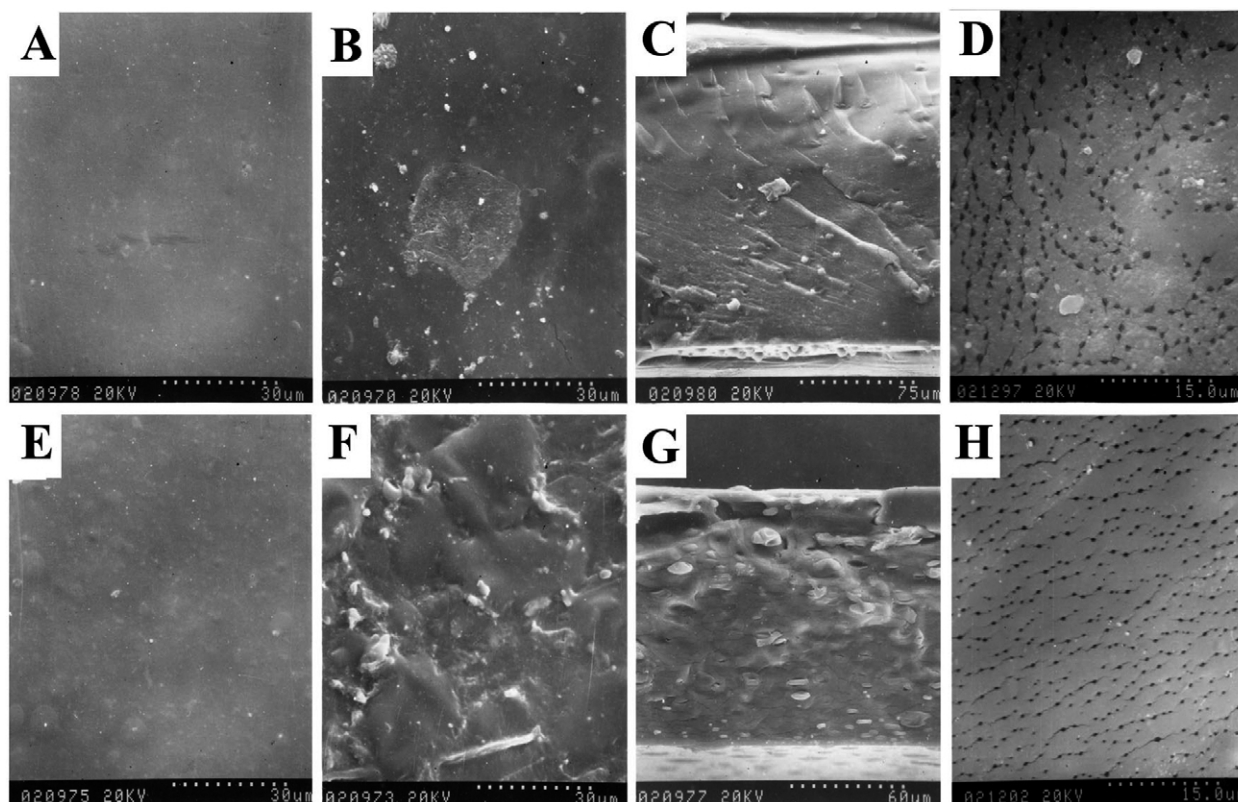


Fig. 2. SEM photographs of the films CMPE65-G (surface side, A; bottom side, B; cross section, C), CMPE65-T (surface side, E; bottom side, F; cross section, G), and the extracted films CMPE65-G (D) and CMPE65-T (H).

calculated by

$$\text{Degree of swelling (wt\%)} = [(w_s - w_0)/w_0] \times 100\% \quad (2)$$

where  $w_s$  represents weight of swelling film. Three parallel measurements were carried out for every sample.

### 3. Results and discussion

#### 3.1. Composition and morphology of films

Infrared spectroscopy can be employed extensively to study the hydrogen bonding based on the frequency shift of the groups. ATR-FTIR spectra of the films WPUE-G, CMPE65-G and CMPE65-T are shown in Fig. 1. For the WPUE-G film the band at  $1725\text{ cm}^{-1}$  was attributed to the stretching of free urethane carbonyl groups, whereas the band centered at  $1603\text{ cm}^{-1}$  was assigned to the stretching of hydrogen-bonded carboxylic carbonyl groups [25–27]. Intensity of peak at  $1725\text{ cm}^{-1}$  decreased, while that of peak at  $1603\text{ cm}^{-1}$  increased for the CMPE films, implying that the intermolecular interactions between CMCH and WPU networks occurred in the CMPE films. A strong absorption peak around  $3330\text{ cm}^{-1}$  caused by the hydrogen bonding between NH and carbonyl groups for the CMPE films appeared, compared with that of WPUE-G ( $3303\text{ cm}^{-1}$ ) [28]. An obvious shoulder peak appeared at  $3285\text{ cm}^{-1}$ ,

corresponding to the  $\text{NH}\cdots\text{O}$  hydrogen bonding between the amide groups of WPU networks and the carboxylic groups of CMCH or the hydroxyls resulted from the epoxide ring opening of EGDE. This implies that the original inter- and intra- molecular hydrogen bonds in the WPU networks were destroyed due to the interpenetrating and entanglements between WPU and CMCH.

The delineation of the ATR-FTIR spectrum for CMPE65-T film at the surface side was almost similar to that at the bottom side, although the intensities of peaks for the surface side are a little higher as compared with that for the bottom side. Whereas in the spectra of CMPE65-G film prepared on the glass, the intensity of peak at  $1725\text{ cm}^{-1}$  for the surface side was markedly less than that for the bottom side, suggesting that CMCH enriched at the surface [29,30]. Moreover, the intensities of peaks at  $3330$  and  $1603\text{ cm}^{-1}$  of the surface side for CMPE65-T film are greater than that for CMPE65-G film, implying that strong hydrogen bonding occurred between WPU and CMCH in the former.

The SEM images of the films extracted with and without water are shown in Fig. 2. The homogeneous morphologies observed on the surface and bottom side of CMPE65-G film suggested that a strong interfacial interaction exist between the glass substrate and the blend components, namely, the affinity between the hydrophilic components and the hydrophilic glass acts as a driving force in order to diminish the interfacial energy at the IPN-substrate interface,

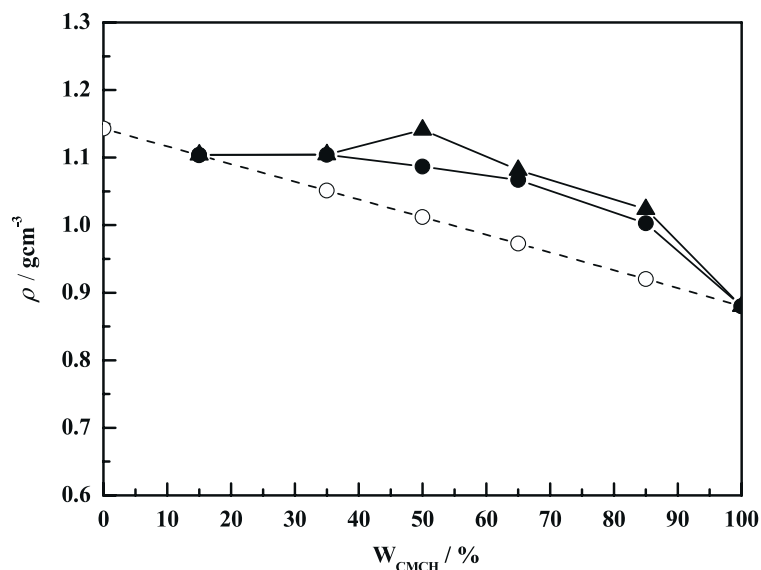


Fig. 3. CMCH content ( $w_{\text{CMCH}}$ ) dependence of the densities from additivity rule (○) and experimental values for the films CMPE-G (●) and CMPE-T (▲).

resulting in the smooth morphology formed at the bottom side [12]. In addition, there is a segregation layer morphology on the cross section of CMPE65-G film (C). This implies that the WPU component preferentially accumulated at the IPN-glass interface and CMCH enriched at the free surface (contact with air), according to the difference in surface tension between WPU and CMCH, similar to that reported by Kano [29]. However, the morphology of CMPE65-T film is slightly different from that of CMPE65-G film. The wave morphology for the bottom side of CMPE65-T film may be caused by repulsion between the hydrophilic components and the hydrophobic substrate. Moreover, the morphology of cross section for CMPE65-T film is relatively homogenous, compared with

that for CMPE65-G film, indicating a relatively dense architecture in inner surface. This implies that strong intermolecular interaction occurred between CMCH and WPU components in the film prepared on the hydrophobic substrate.

Water is a good solvent of CMCH, while the cross-linked WPU is basically insoluble in this case. Thus the distribution of CMCH in the CMPE films can be obtained from the films extracted with water to remove the CMCH. The SEM photographs of the extracted films are also shown in Fig. 2 (D and H). The black domain is the void, where the water-soluble CMCH was removed. Seemingly, cross-linked WPU formed a continuous phase and CMCH as a dispersed phase. The surfaces of extracted films CMPE65-G

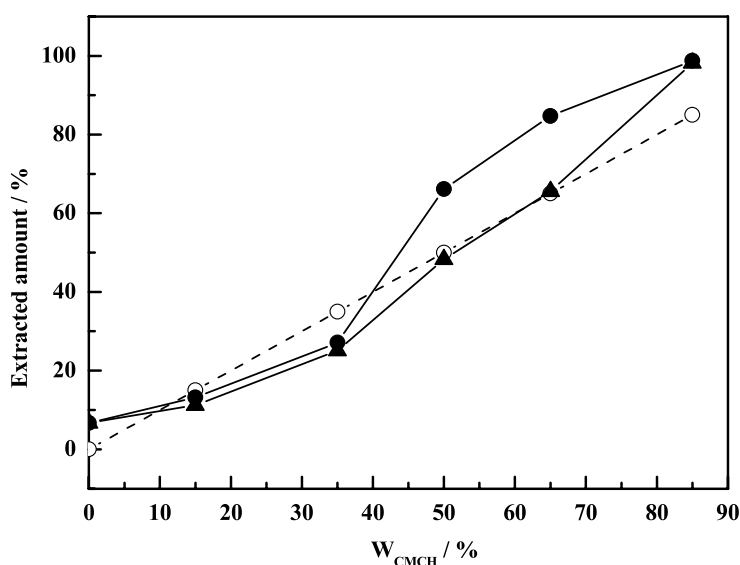


Fig. 4. CMCH content ( $w_{\text{CMCH}}$ ) dependence of the theoretical (○) and experimental amounts of CMCH extracted with water from the films CMPE-G (●) and CMPE-T (▲).



and CMPE65-T all exhibited homogeneous distribution of the porous, in which the CMCH was removed from WPU networks in the films, suggesting a good or certain level of miscibility between CMCH and WPU networks. Furthermore, the SEM micrographs revealed that the average size of the voids for CMPE65-T film is smaller than that for CMPE65-G film, but the number of voids per unit area for the former is much more than that for the latter. It is indicated that the CMCH macromolecules more easily penetrated into WPU networks to form stronger intermolecular interaction in the semi-IPN films with Teflon as substrate than that with glass as substrate [31]. In addition, this result further confirmed that the relatively large CMCH amounts exist on the free surface, which dissolved more easily in water for CMPE65-G film. In review of ATR-FTIR and SEM analysis of CMPE films, the relatively strong intermolecular interaction between WPU and CMCH occurred in the CMPE-T films. This can be explained that two kinds of hydrophilic macromolecules all escaped from the surface of hydrophobic substrate to aggregated toward each other to form a relatively homogenous and dense structure in the CMPE-T films.

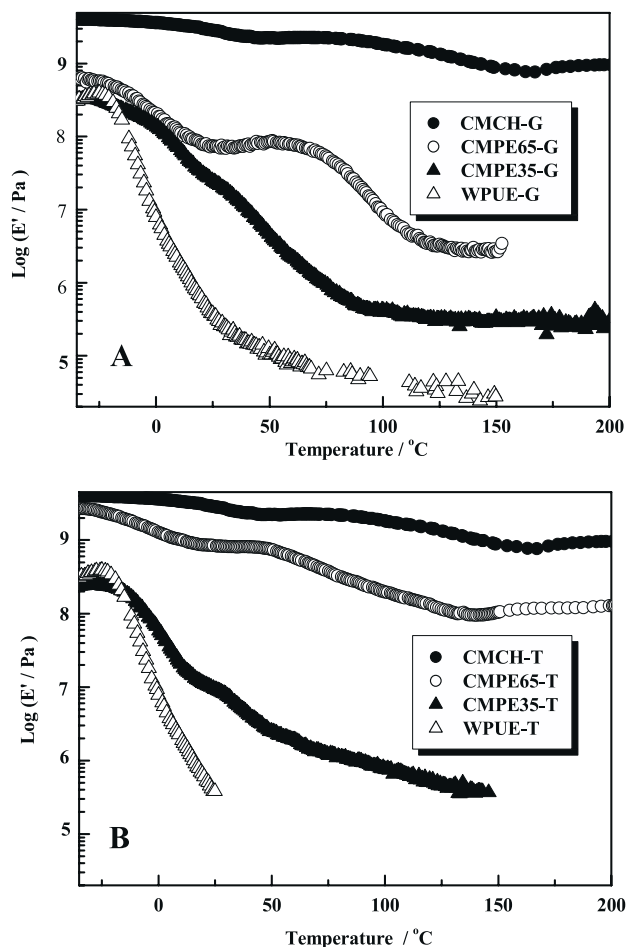


Fig. 5. Storage modulus ( $E'$ ) as a function of temperature for the films CMPE-G (A) and CMPE-T (B).

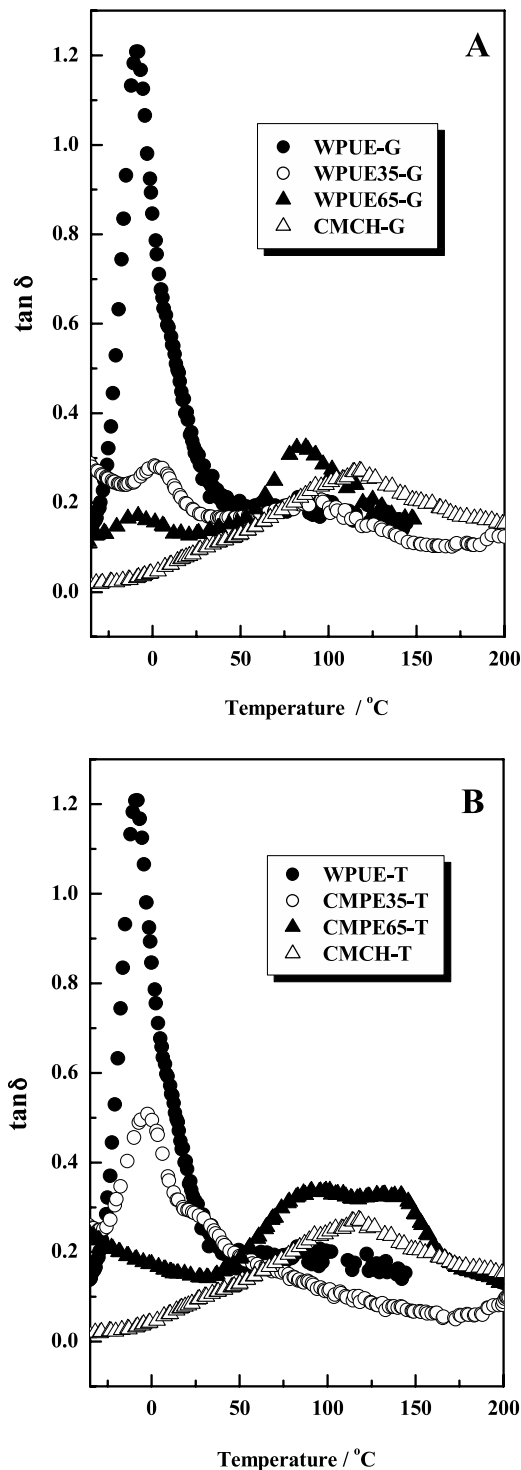


Fig. 6.  $\tan \delta$  as a function of temperature for the films CMPE-G (A) and CMPE-T (B).

### 3.2. Miscibility between WPU and CMCH

The densities measured from the volume density of the components as a function of CMCH content are shown in Fig. 3. In a polymer blend, where there is no adhesion between the polymer interface and no molecular mixing at

the phase boundary, the density of the blend would be expected to follow the additivity rule of mixtures [32]. In the CMPE films, all of the experiment values of density are obviously higher than that calculated, further indicating that a strong adhesion exists between WPU networks and CMCH molecules. This implies that CMCH molecules penetrated into WPU networks to bind together, led to a reduction of the free volume of the semi-IPN films. In addition, the CMPE-T films possessed higher densities than that of the CMPE-G films, revealing that the films prepared with the Teflon as the substrate have more dense structure than that with the glass as the substrate.

The CMCH amounts extracted with water as a function of CMCH content for the films CMPE-G and CMPE-T are shown in Fig. 4. When CMCH content were more than 35 and 65 wt%, respectively, the extracted CMCH amounts of the films CMPE-G and CMPE-T were higher than the theoretical values, indicating that excessive amount of CMCH hindered the WPU network formation. This suggests that a small quantity of WPU was removed, because water is a good solvent for both CMCH and uncross-linked WPU. When CMCH content in the films CMPE-G and CMPE-T were less than 35 and 65 wt%, respectively, the extracted CMCH amounts were lower than the theoretical values, implying that strong intermolecular bonding and entanglement between CMCH and WPU networks to prevent the dissolution of CMCH from WPU networks, similar to the results of poly(vinyl chloride) and oligomeric MDI isocyanate cross-linked networks reported by Pittman Jr et al. [33]. Therefore, the films CMPE-G and CMPE-T containing CMCH content lower than 35 and 65 wt%, respectively, have the relatively complete WPU networks. Moreover, the results revealed that extracted CMCH amounts of CMPE-G films were higher than that of CMPE-T films, due to the dissolution of CMCH enriched on the free surface.

The storage modulus ( $E'$ ) and mechanical loss factor ( $\tan \delta$ ) of the films as a function of temperature are shown in Figs. 5 and 6. The storage moduli of CMCH in the rubbery state could not be obtained because it will be degraded when the temperature was above 200 °C. The  $E'$  values of the films WPUE, CMPE35-G and CMPE35-T decreased dramatically with an increase of temperature, and the films CMCH and CMPE65-T had high storage modulus even when the temperature was above 200 °C. However, the storage moduli for CMPE65-G film significantly decreased as the temperature was above 80 °C. Interestingly, the storage modulus of the CMPE-T films significantly increased as CMCH content increased from 35 to 65 wt%. Ishida et al. have reported that stiffness is related to changes of the stored elastic energy in the glassy state [34]. The  $E'$  value of the CMPE65-T film was higher than that of the CMPE65-G film in the glassy state, suggesting that the CMPE65-T film appeared more able to resist segmental motion. This can be explained that CMPE65-T film possessed more complete WPU networks and stronger

interaction between CMCH and WPU than that of CMPE65-G film mentioned above.

Usually, the  $\alpha$ -relaxation,  $\tan \delta$  peak, reflects the glass transition, and may be analyzed to provide information about the motion of molecules. If the two starting materials had phase separation and prevented interaction, there are two glass transition peaks for the blends.  $T_g$  corresponding to PU soft segment was measured to be around  $-10$  °C and that to CMCH at 120 °C as shown in Fig. 6. There is one loss peak for the film CMPE35-T, implying a good miscibility between WPU networks and CMCH. However, two loss peaks corresponding to each component were observed for CMPE65-G film. The damping peaks of both components for CMPE65-G film shifted toward each other, indicating that the CMPE65-G film is miscible in certain degree. Interestingly, a broad prominent damping peak corresponding to the CMCH in the CMPE65-T film reflects toughness and multi-molecular motion of the polymer material, which was prescribed to increase miscibility of the components. The results confirmed that WPU networks and CMCH have

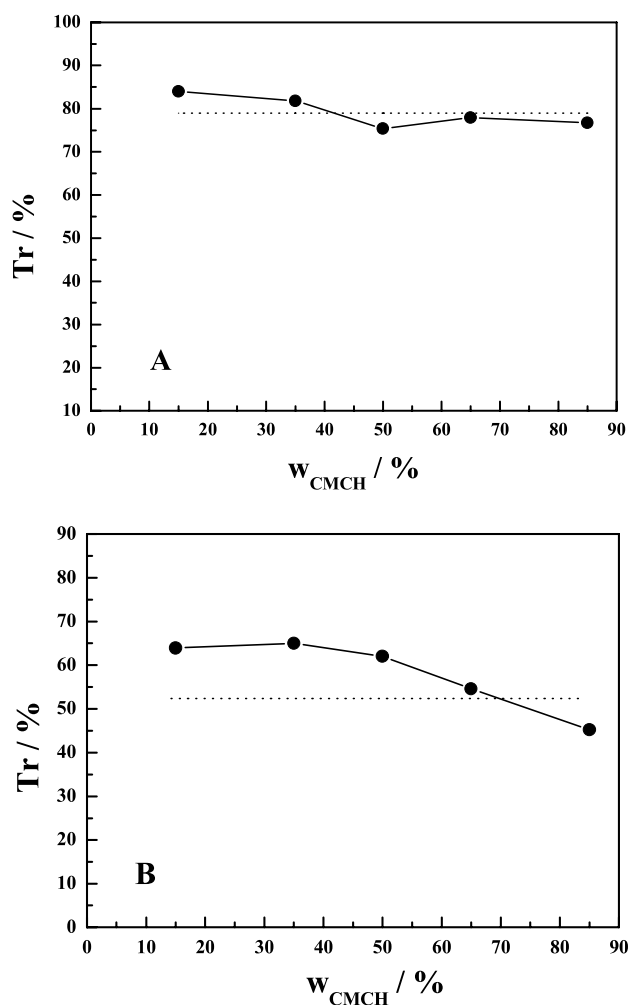


Fig. 7. CMCH content ( $w_{\text{CMCH}}$ ) dependence of light transmittance ( $T_r$ ) at 800 nm of the films CMPE-G (A) and CMPE-T (B). Mark ( $\cdots$ ) presents the  $T_r$  values of the WPUE films prepared on the glass and Teflon, respectively.

better miscibility over the entire composition range studied here for CMPE-T films than that of the CMPE-G films. These findings supported the conclusions obtained by ATR-FTIR, SEM and density measurement. Furthermore, the height and width of the  $\alpha$ -relaxation peak can be used to analyze the trend of molecular motion of cross-linking polymers. The decreasing height and broadening width of the  $T_g$  peak related to WPU soft segment for the CMPE65-T film is associated with lower segmental mobility and thus is indicative of a higher degree of cross-linking for the blends [34].

In addition, the transparency of the films is an auxiliary criterion to judge the miscibility of the composite materials [35]. Dependence of the light transmittance ( $T_r$ ) on the CMCH content for the films CMPE-G and CMPE-T are shown in Fig. 7. The  $T_r$  values of CMPE-T films (B) are higher than that of WPUE-T film except for CMPE85-T film, while  $T_r$  values of CMPE-G films (A) changed hardly compared with that of WPUE-G film. The enhancement in  $T_r$  of the CMPE-T films can be explained that interfacial adhesion between two kinds of macromolecules with small-dispersed phase domain in the semi-IPN structure is very intimate. These results clearly revealed that the solid substrate could also greatly influence the miscibility between the components.

### 3.3. Thermal and mechanical properties of films

Thermal degradation patterns of the films are shown in Fig. 8. A small weight loss at 25–200 °C was assigned to the release of moisture and TEA from the samples. The weight losses at 300–500 °C were believed to be caused by oxidation and degradation. Generally, the thermal degradation of semi-IPN in dynamic conditions and in the presence of oxygen shows three decomposition stages [36]. The degradation onset temperature ( $T_{10}$ ) of the CMPE films is around 300 °C (start for the first stage), and an increasing decomposition rate is observed between 350 and 500 °C (the second stage) when the weight losses reached about

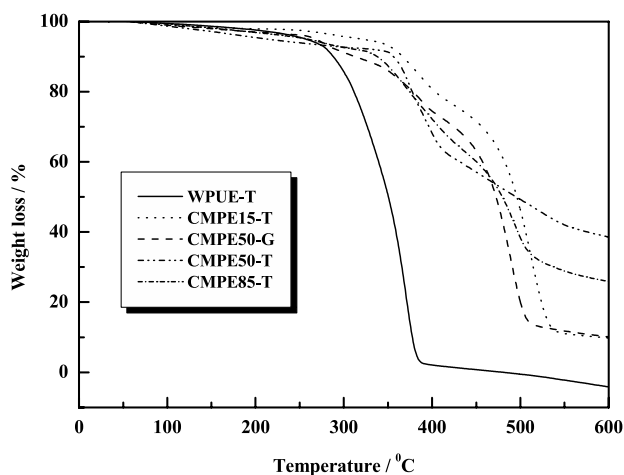


Fig. 8. TGA thermograms of the films under an air atmosphere.

Table 1  
Thermal behavior of the films

Samples	$T_{10}$ (°C)	$T_{50}$ (°C)	$T_m$ (°C)	$T_i$ (°C)	Residue at 600 °C (wt%)
WPUE-T	288	350	359	109	0.03
CMPE15-T	366	495	506	114	9.87
CMPE50-G	314	471	482	110	10.44
CMPE50-T	357	480	575	103	38.87
CMPE85-T	313	499	497	110	25.97

60–70 wt%. The third stage of decomposition for temperatures are higher than 500 °C corresponding to the advanced fragmentation of the chain formed in the first and second stages of decomposition, as well as to the secondary reactions of dehydrogenation and gasification processes. Almost complete decomposition was observed at 600 °C. Data related to the temperature corresponding to 10 wt% ( $T_{10}$ ) and 50 wt% ( $T_{50}$ ) weight loss of the initial weight, as well as the temperature taken for the maximum rate of decomposition ( $T_m$ ) along with initial decomposition ( $T_i$ ), and residues at 600 °C are summarized in Table 1. The semi-IPN films exhibited much higher thermal stability than that of

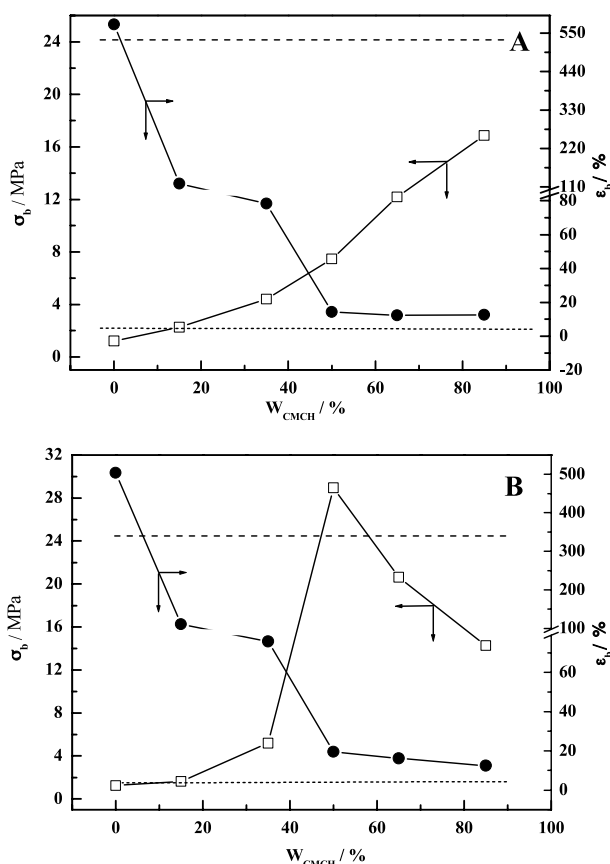


Fig. 9. CMCH content ( $w_{\text{CMCH}}$ ) dependence of tensile strength ( $\sigma_b$ ,  $\square$ ) and elongation at break ( $\epsilon_b$ ,  $\bullet$ ) of the films CMPE-G (A) and CMPE-T (B). Mark (—) and (···) represent  $\sigma_b$  and  $\epsilon_b$  of the CMCH films prepared on the glass and Teflon, respectively.



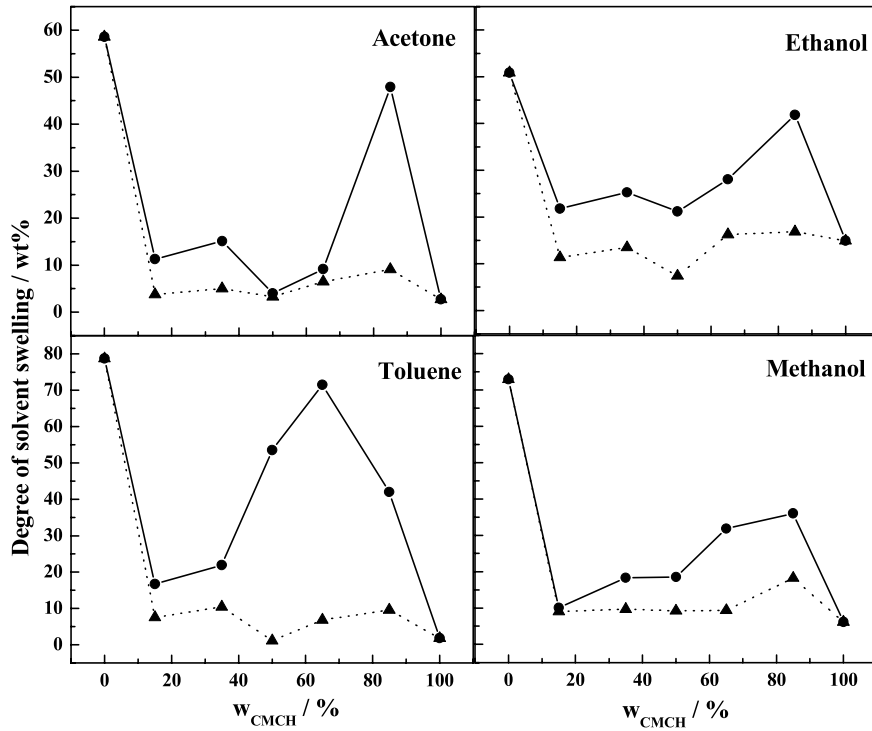


Fig. 10. CMCH content ( $w_{CMCH}$ ) dependence of the degree of solvent swelling for the films CMPE-G (●) and CMPE-T (▲).

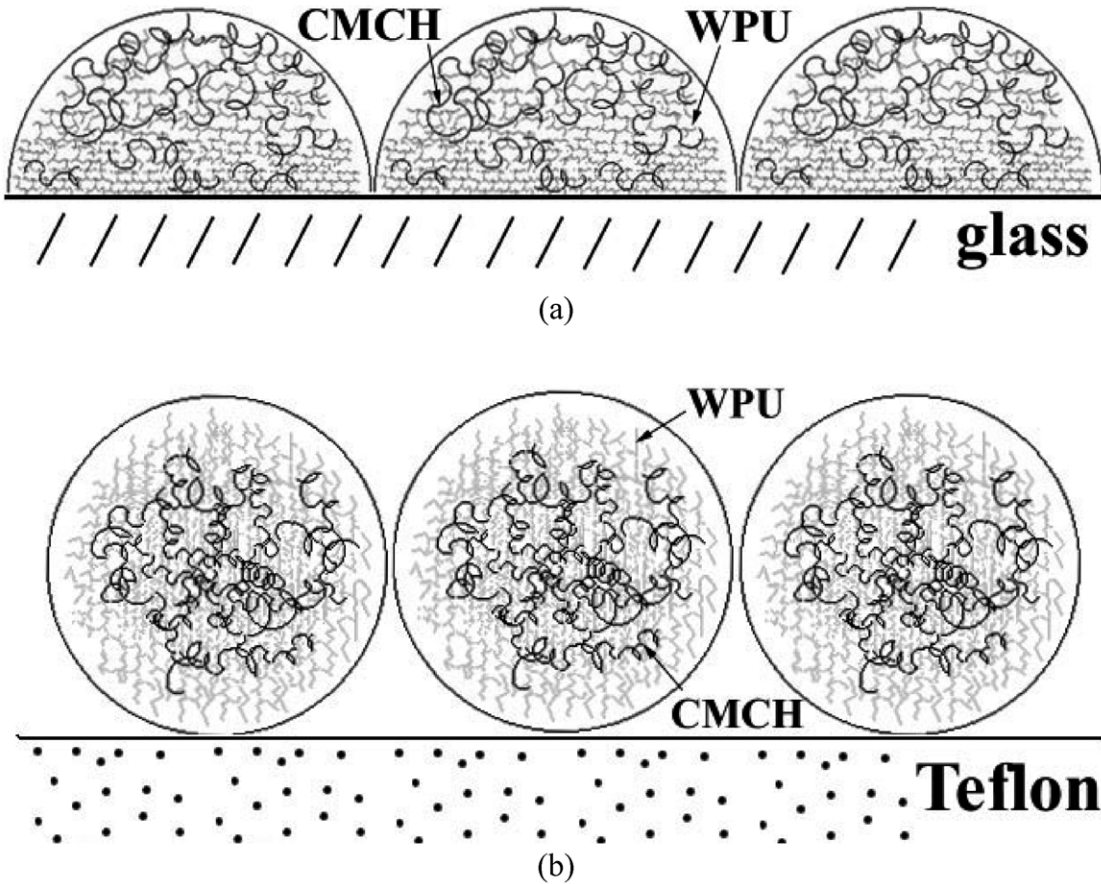


Fig. 11. Schematic diagrams of the model describing the formation of WPU/CMCH semi-IPN films on the glass (a) and Teflon (b) mold.

WPUE film, implying that an enhancement of thermal stability caused by strengthening of CMCH as well as interaction between WPU and CMCH. Moreover, the residue at 600 °C of CMPE50-T film (38.87%) is higher than that of CMPE50-G film (10.44%), also suggesting more effective reinforcement and strong interaction of two kinds of molecules in the films prepared on the Teflon than that on the glass.

The CMCH content dependence of the tensile strength ( $\sigma_b$ ) and elongation at break ( $\epsilon_b$ ) for the films CMPE-G and CMPE-T are shown in Fig. 9. The  $\sigma_b$  values for the CMPE-G films increased from 2.26 to 16.86 MPa with an increase of CMCH content from 15 to 85 wt%. Interestingly, the tensile strength of the CMPE-T films increased with increasing CMCH content up to a maximum value (28.95 MPa) for CMPE50-T film, and then decreased with the continued increase of CMCH content in the semi-IPN film. This result implies that the film CMPE50-T containing 50 wt% CMCH have both more complete cross-linking networks, which were proved by following solvent swelling results shown in Fig. 10, and stronger interaction between CMCH and WPU than others. Moreover, the tensile strength of the CMPE-T films are significantly higher than that of the CMPE-G films. The improvement in the tensile strength could be resulted from an enhancement in interpenetration and the interaction between WPU and CMCH molecules. In addition, solvent swelling and solvent resistance tests are good methods to determine the quality of the density of the semi-IPN materials. As cross-linking intensity increases, the ability of the composites to swell in the solvent decreases. Fig. 10 shows the results from solvent-resistance tests for 24 h. The solvent-resistance of the CMPE films increased with an increase of CMCH content, and the CMPE-T films appeared higher chemical resistance than the CMPE-G films. In particular, the CMPE50-T film has the excellent chemical resistance, attributing to its higher cross-linking density.

### 3.4. Effects of solid substrate on casting film

In review of the results mentioned above, the CMPE-T films possessed better miscibility and higher density, storage modulus, thermal stability and tensile strength than the CMPE-G films over the entire composition range. This is due to that the more uniform and dense architecture caused by stronger interaction between WPU and CMCH in the films prepared on the Teflon than that on the glass. A model describing the formation of the hydrophilic WPU/CMCH semi-IPN film cast on the different solid substrate was proposed to illustrate the differences of their structures and properties as shown in Fig. 11. The glass substrate is known to thermodynamically favor contact with hydrophilic polymers and ionic monomers [16]. As shown in Fig. 11(a), a segregation morphology for the CMPE-G film formed in inner, owing to that the strong affinity between the hydrophilic components and the hydrophilic

substrate acted as a driving force to diminish the interfacial energy, attracting of the components to the surface of glass substrate. Meanwhile, surface segregation in polymer blends occurs as a low surface tension WPU component is preferentially enriched at the polymer-substrate interface according to the difference in surface tension of the components. As a result, a relatively loose architecture of the CMPE-G films appeared in the inner surface. On the contrary, the CMPE-T film had a uniform and densely packed architecture as shown in Fig. 11(b). The hydrophilic WPU and CMCH were more readily forced to interpenetrate together, owing to that two kinds of macromolecules all were repulsed from the Teflon surface to concentrate into inner surface.

## 4. Conclusions

Two series of semi-IPN films from cross-linked water-borne polyurethane and carboxymethylchitin were successfully prepared on the hydrophilic and hydrophobic substrates of glass and Teflon, respectively. The results revealed that the semi-IPN films had higher light transmittance, thermal stability and tensile strength than WPU film, suggesting good miscibility when CMCH content was lower than 35 and 65 wt% for the films CMPE-G and CMPE-T, respectively. It was worth noting that the CMPE-T films exhibited better miscibility and higher density, storage modulus, thermal stability and tensile strength than that of the CMPE-G films over the entire composition range studied here. This difference can be attributed to stronger entanglement and interaction between WPU and CMCH macromolecules in the CMPE-T films than that in the CMPE-G films. The structure, miscibility and properties of the hydrophilic semi-IPN films depended significantly on the solid substrates, and using the hydrophobic solid substrate can effectively improve the miscibility and properties of the casting semi-IPN films with hydrophilic character. A model describing the formation and structure of hydrophilic WPU/CMCH semi-IPN films cast on the hydrophilic and hydrophobic substrates was proposed here to illustrate the effect of the substrates.

## Acknowledgements

This work was supported by Major Grant of the National Natural Science Foundation of China (59933070).

## References

- [1] Muzzarelli RAA. Chitin. New York: Pergaman Press; 1977. Chapter 1.
- [2] Migashita Y, Kobayashi R, Nishio Y. Carbohydr Polym 1997;34(4): 221–8.

- [3] Williamson SL, Porter RS, McCormick CL. *Macromolecules* 1998;31(23):8134–41.
- [4] Hjerde RJNH, Varum KM, Grasdalen H. *Carbohydr Polym* 1997;34(3):131–9.
- [5] Nishimura S, Nishi N, Tokura S. *Carbohydr Res* 1986;146(2):251–8.
- [6] Duecoffre V, Diener W, Flosbach C, Schubert W. *Prog Org Coat* 1998;34(1–4):200–5.
- [7] Brinkman E, Vandevoorde P. *Prog Org Coat* 1998;34(1–4):21–5.
- [8] Coogan RG. *Prog Org Coat* 1997;32(1–4):51–63.
- [9] Ley DA, Fiori DE, Quinm RJ. *Prog Org Coat* 1999;35(1–4):109–16.
- [10] Coleman MM, Zarian J. *J Polym Sci: Polym Phys* 1979;17(5):837–50.
- [11] Thomas DA, Sperling LH. *Polymer blends*, vol. 2. New York: Plenum Press; 1979.
- [12] Sperling LH. *Interpenetrating polymer networks and related materials*. New York: Plenum Press; 1981.
- [13] Gao S, Zhang L. *Macromolecules* 2001;34(7):2202–7.
- [14] Lu Y, Zhang L. *Polymer* 2002;43(14):3979–86.
- [15] Zhang L, Zhou Q. *J Polym Sci: Polym Phys* 1999;37(14):1623–31.
- [16] Lipatov YS. *Prog Polym Sci* 2002;27(9):1721–801.
- [17] Lipatov YS. *Polymer* 1999;40(23):6485–92.
- [18] Turner JS, Cheng YL. *Macromolecules* 2000;33(10):3714–8.
- [19] Oslanec R, Brown HR. *Macromolecules* 2001;34(26):9074–9.
- [20] Kim YS, Kim SC. *Macromolecules* 1999;32(7):2334–41.
- [21] Zeng M, Zhang L, Wang N, Zhu Z. *J Appl Polym Sci* 2003;90(5):1233–41.
- [22] Delpech MC, Coutinho FMB. *Polym Test* 2000;19(8):939–52.
- [23] Hepburn C. *Polyurethane elastomers*. New York: Applied Science Publishers; 1982. p. 290.
- [24] Muzzarelli RAA. *Carbohydr Polym* 1988;8(1):1–21.
- [25] Wen TC, Wu MS. *Macromolecules* 1999;32(8):2712–20.
- [26] Teo LS, Chen CY, Kuo JF. *Macromolecules* 1997;30(6):1793–9.
- [27] Wen T, Wang Y, Cheng T, Yang C. *Polymer* 1999;40(14):3979–88.
- [28] Miller JA, Lin SB, Cooper SL. *Macromolecules* 1985;18(1):32–44.
- [29] Kano Y, Inoue M, Akiba I. *Polymer* 1998;39(26):6747–54.
- [30] Yin W, Gu T. *Polymer* 1997;38(20):5173–8.
- [31] Agari Y, Shimada M, Ueda A, Nagai S. *Macromol Chem Phys* 1996;197(6):2017–33.
- [32] Kim SC, Klempner D, Frisch HL. *Macromolecules* 1976;9(2):258–63.
- [33] Pittman Jr CU, Xu X, Wang L, Toghiani H. *Polymer* 2000;41(14):5405–13.
- [34] Ishida H, Allen DJ. *Polymer* 1998;39(19):4487–95.
- [35] Krause S. *J Macromol Sci: Rev Macromol Chem* 1972;7(2):251–73.
- [36] Cascaval CN, Rosu D, Rosu L, Ciobanu C. *Polym Test* 2003;22(1):45–9.